ELECTROPHYSIOLOGICAL PROPERTIES OF CRAYFISH RETINAL PHOTORECEPTORS

By ARTURO PICONES and HUGO ARÉCHIGA

Departamento de Fisiología, Biofísica y Neurociencias, Centro de Investigación y de Estudios Avanzados del IPN, México, DF

Summary

Electrical properties of crayfish retinular photoreceptors were studied in the dark-adapted state and during responses to light. In fully dark-adapted photoreceptors, the resting potential was -49.8 ± 3.3 mV and input resistance was 31.3 ± 5.4 MΩ (mean±s.e.). The current–voltage relationship showed rectification near the resting potential, with decreased resistance within the depolarizing range. A value of 29.8 ± 5.0 kΩcm^2 was calculated for specific resistance, and 3.0 ± 0.4 μF cm^{-2} for specific capacitance. Electrotonic analysis showed that the photoreceptor was isopotential.

During the light response, membrane conductance increased depending on the stimulus intensity. This relationship was steeper for the conductance change during the initial transient of the receptor potential than during the plateau. A depolarizing afterpotential usually ensued at the end of the light response, concurrent with a residual increased conductance. The time course of the conductance increase during the receptor potential showed two kinetic components, suggesting that at least two distinct membrane processes were involved in its generation.

Introduction

Crayfish retinular cells respond to light with a slow, graded depolarization, the receptor potential (RP). The time course and intensity-dependence of the RP have been amply studied (Glantz, 1968; Laughlin, 1981), but its nature is not yet fully understood (Fain and Lisman, 1981; Cummins and Goldsmith, 1986). It is probably generated by a light-induced increase of ionic membrane conductance(s) similar to that characterized for other arthropod photoreceptors (Shaw and Stowe, 1982), but there is no direct evidence for this. Conductance changes have either been assumed (Glantz, 1968, 1972; Stieve *et al.* 1971) or been determined only for strong intensities of illumination (Stieve *et al.* 1977; Cummins and Goldsmith, 1986). An interaction between light and the activity of a Na^+,K^+-ATPase system has also been proposed as an integral part of the phototransduction mechanism in crustaceans (Fain and Lisman, 1981). Likewise, no appropriate characterization

has been made of the passive membrane electrical properties of the retinular cells. Information on the membrane electrical properties of these receptors is particularly relevant to any explanation of the membrane mechanisms underlying the various modulatory influences known to affect crustacean retinal responsiveness, such as the circadian rhythm of sensitivity to light (Aréchiga and Huberman, 1980; Bryceson, 1986) and the effect of neuromodulators on photoreceptor responsiveness (Aréchiga et al. 1990). The purpose of this work is to characterize the electrical properties of crayfish retinular cells, in darkness and during the response to light pulses.

A preliminary report of these results has been published in abstract form (Picones and Aréchiga, 1985).

Materials and methods

Experiments were conducted on adult crayfish *Procambarus clarkii*, of either sex and in intermoult. Animals were dark-adapted for 2–4 h before the dissection procedure. All recordings were made during the afternoon and night. The eyestalks were removed under dim red illumination and bisected longitudinally with a razor blade to allow direct access to the photoreceptor layer. In some experiments the retina with the lamina ganglionaris was dissected away from the rest of the eyestalk structures. The eye was mounted in a transparent perfusion chamber and immersed in van Harreveld's solution (ionic concentration in mmol l^{-1}: NaCl, 205; KCl, 5; CaCl$_2$, 14; MgCl$_2$, 3; Hepes–Na$^+$ buffer, 2; pH adjusted to 7.4). The bath temperature was kept constant at 17–19°C using a Peltier device. The preparation was left in the dark for at least 15 min before the recording procedure.

The microelectrodes were pulled from microfibre borosilicate glass capillary tubes, filled with 3 mol l^{-1} KCl solution. Their resistance ranged from 50 to 90 MΩ. Voltage recording and current injection were done with a WP-Instruments KS700 bridge amplifier. The electrical signals were stored in an FM instrumentation tape recorder (Vetter) and displayed on an oscilloscope (Tektronix) and/or a pen recorder (Gould). The amplifier probe with the microelectrode was mounted on a hydraulic microdrive and attached to a mechanical micromanipulator (Narishige).

Light pulses were delivered from a microscope lamp (Nikon). Intensity was regulated with neutral density filters (Kodak Wraten no. 96). Light-pulse duration was set with an electromechanical shutter (Alphax Syncromatic) and monitored with a photocell adapted to the optical axes of the observing microscope. The light-pulse intensity was calibrated with a Gossen Lunasix 3 photometer.

Experimental procedure

Under dim red light the electrode tip was placed on the photoreceptor layer. The red light was then turned off and the electrode was slowly and gently advanced through this layer. Impalements were aided either by gentle taps or by brief

oscillations produced with the capacity compensation circuit. It was assumed that the microelectrode had penetrated a retinular cell when the following criteria were attained: (i) a sudden drop to a stable negative resting potential (V_{rest}), (ii) a capacitative transient in the voltage deflection for hyperpolarizing current pulses applied through the microelectrode and (iii) a depolarizing response to illumination. Anatomical observations show that the only other type of cells present is accessory pigment cells, which are not responsive to light (Naka and Kuwabara, 1959). The results reported in this paper were obtained from 22 photoreceptors for which a complete analysis of electrophysiological properties was made, which required at least 40 min of stable intracellular recording.

The membrane input resistance (R_{in}) was calculated by linear regression of the current–voltage (I–V) relationship at the steady-state level of voltage deflection (V_∞) from V_{rest} for hyperpolarizing current pulses.

Results

The photoresponse

Light-induced electrical responses were analysed within the range 10^0–10^4 lx. A series of recorded RPs and the corresponding stimulus–response relationship (V–log$I$ curve) for a representative photoreceptor from our sample is shown in Fig. 1. Confirming earlier descriptions (Eguchi, 1965; Glantz, 1968; Nosaki, 1969; Waterman and Fernández, 1970; Muller, 1973; Stieve *et al.* 1976; Cummins and Goldsmith, 1981; Bryceson, 1986), our results showed two conspicuous features of the RP: (a) an initial transient depolarization and (b) a subsequent plateau at a lower level. In some cases, for high intensities, these two components were separated by a more or less pronounced dip (data not shown), as observed in other invertebrate photoreceptors (see Fuortes, 1963; Naka and Eguchi, 1962). These two components had different thresholds, that of the initial transient component being about half a log unit higher than that for the plateau. Typically, the RP was followed by a depolarizing afterpotential (DAP), which lasted for some seconds (see below). The V–log$I$ relationship for the initial transient can be fitted by the following rectangular hyperbola equation:

$$V = V_{max}\frac{I^n}{I^n + I_o},\tag{1}$$

where V is the voltage amplitude in response to a given light intensity I, V_{max} is the saturated response amplitude, I_o is the half-saturation intensity constant and n is an exponent that accounts for a second non-linearity in the summation process (Glantz, 1972; Laughlin, 1981), also known as the Hill coefficient. The procedure used to fit equation 1 to the experimental data was accomplished using the Simplex algorithm (Caeci and Cacheris, 1984).

Equation 1 was originally used by Naka and Rushton (1966) for fish photoreceptors and subsequently applied to many other types of photoreceptors, among them
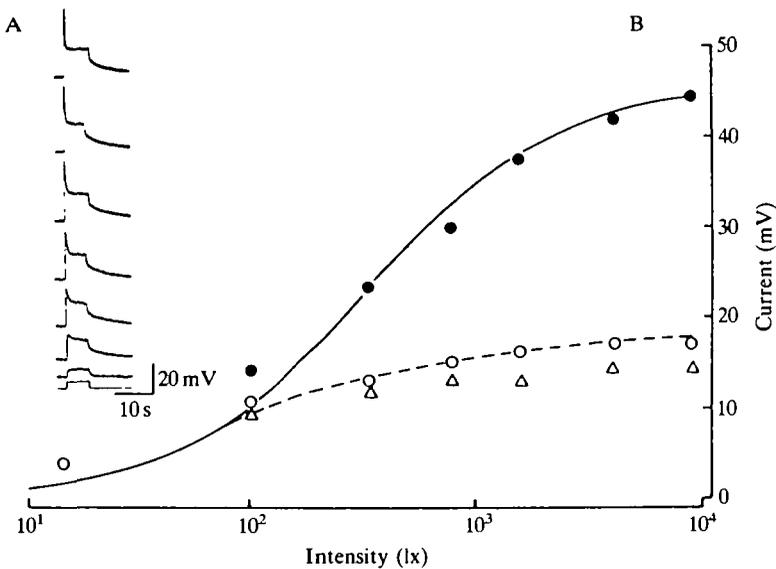
Fig. 1. Stimulus–response relationships for the receptor potential phases. (A) Intra-cellular recording of the receptor potential (RP) of a retinal cell in response to increasing light intensity. The stimuli were rectangular pulses (photocell record at bottom) of diffuse white light within the range of intensities shown in B. (B) V–log$I$ curves of the initial transient wave (●), the late plateau (○) and the prolonged depolarizing afterpotential (△) for the records shown in A. The continuous line fitted to the transient is calculated from equation 1 (see text), using $n=1.02$, $I_o=368.0$ lx and $V_{max}=45.9$ mV. The dashed line is the best line fitting the plateau values. $V_{rest}=-55$ mV, $t=18°$C.

those of *Procambarus clarkii* (Glantz, 1968). Its adequacy to describe our experimental points on the V–log$I$ curve is evident.

The ranges of the parameters of the equation covered by our cell sample were: 35–50 mV for V_{max}; 200–600 lx for I_o in fully dark-adapted photoreceptors; and the value of n was usually close to 1.0.

The intensity function for the initial transient phase of the RP was much steeper than that for the later plateau and the DAP (Fig. 1). Again, this is in agreement with results from other invertebrate photoreceptors (see Shaw and Stowe, 1982).

Passive electrical properties in the dark

The values taken for V_{rest} correspond to those observed in full dark adaptation. A protocol of hyperpolarizing–depolarizing constant-current pulses was followed. Constant-current pulses were made long enough to charge the membrane capacitance completely (injecting current until a well-defined constant level was reached in the voltage deflection). Voltage change was determined in the steady-state part of the voltage deflection. All the electrotonic analysis was made within the linear range of the electrode resistance (up to ±1 nA of injected current). The I–V relationships of three dark-adapted photoreceptors are shown in Fig. 2. A
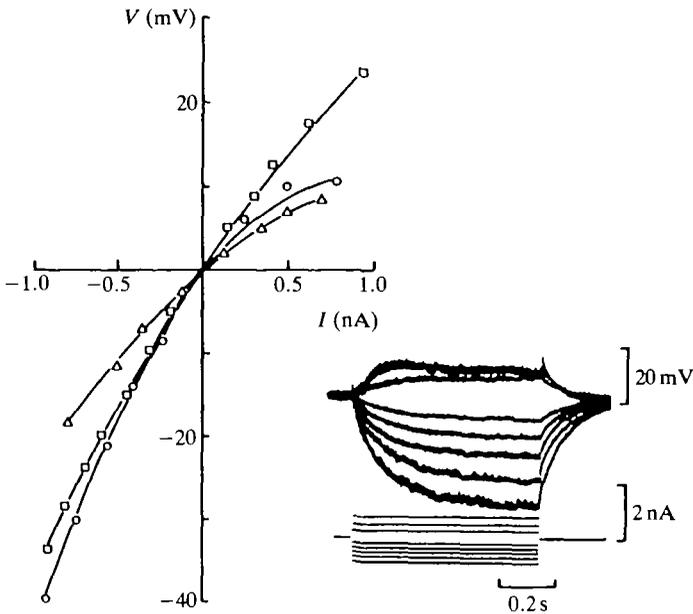
Fig. 2. Steady-state current–voltage relationship of three representative photoreceptors. The inset shows the voltage and current records for the photoreceptor represented by the circles. The ordinate represents the steady-state level of the voltage deflection from V_{rest}.

was greater in the hyperpolarizing range, $31.3\pm5.4\,M\Omega$, than in the depolarizing range, $19.2\pm3.9\,M\Omega$.

The method used for the electrotonic analysis is illustrated in Fig. 3 for the linear hyperpolarizing range of the I–V curves. As a first approximation, this analysis was performed by semilogarithmic plotting of the voltage deflection, measured as the difference between the steady-state level (V_∞) and each point of the voltage transient (V_t). The curve followed a simple exponential (Fig. 3A), as for a circuit of resistance and capacitance in parallel. The membrane time constant (τ_m) was calculated as the negative reciprocal value for the slope of the linear regression fitted to the experimental points of this plot. In a more rigorous way, the time course of the slope of the charging function (dV/dt) was examined with a semilogarithmic plot using the normalized time variable T (t/τ_m) for comparative purposes (Fig. 3B). This second approach showed again that a single exponential component was sufficient to describe the decay of the voltage transient and, therefore, that the cell reacted as an isopotential compartment. Accordingly, the various passive electrical parameters were calculated for the whole photoreceptor sample and their mean values are summarized in Table 1. Total capacitance was derived from the value of τ_m divided by the value of R_{in}. The specific resistance or membrane resistivity (R_m) and the specific capacitance (C_m) were calculated using the estimated value for the cell membrane surface area of the soma, the
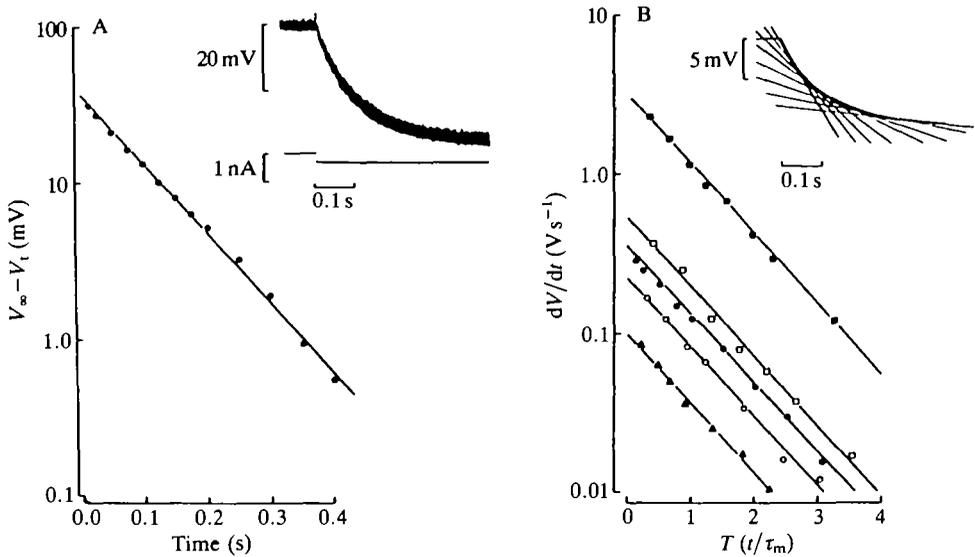
Fig. 3. Electrotonic analysis using a negative current pulse. (A) The ordinate represents the voltage charging curve, measured as the difference between the steady-state level (V_∞) and each point of the voltage transient (V_t). The inset shows the current pulse (bottom trace) and the voltage deflection (top trace) used. τ_m (the membrane time constant)$=98$ ms. (B) Time course of the charging function (dV/dt) for five different photoreceptors. Abscissa: the normalized time variable T (t/τ_m). The inset shows the voltage deflection and the superimposed tangents used to construct the curve. This display corresponds to the solid circles. Note that a single exponential curve can describe the time decay in all the cases exemplified. The τ_m values for each case are 15 (■), 53 (□), 98 (●), 91 (○) and 102 ms (▲).

Table 1. *Electrical parameters of crayfish retinular cells under dark adaptation*

Resting potential (mV)	-49.8 ± 3.3
Input resistance (MΩ)	31.3 ± 5.4*
Time constant (ms)	79.0 ± 9.8
Total capacitance (nF)	3.2 ± 0.5
Specific resistance (kΩcm^2)	29.8 ± 5.0
Specific capacitance (μF cm^{-2})	3.0 ± 0.4

Values are the mean$\pm$s.e. of 22 individual photoreceptors.
* Linear regression for hyperpolarizing pulses.

rhabdomeric microvilli and the photoreceptor axon ($91\,000\,\mu$m^2, taken from Krebs, 1974).

Membrane conductance changes in response to illumination

As anticipated, during the RP an increase in membrane conductance (G_m) was
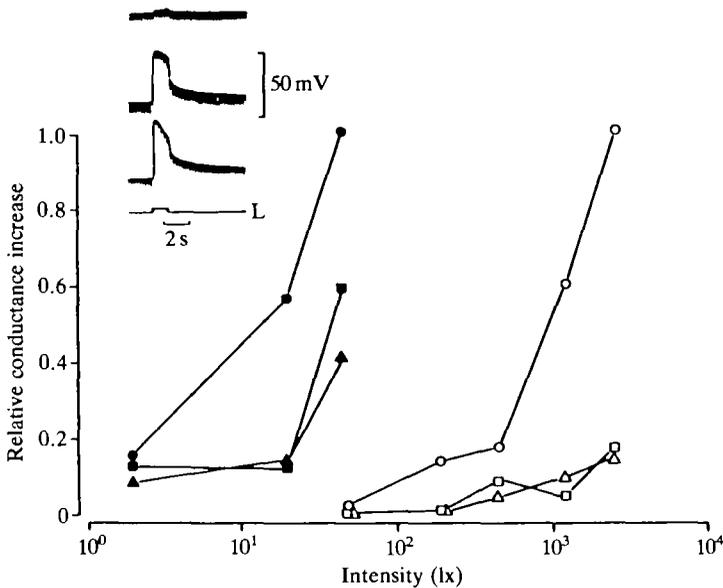
Fig. 4. Stimulus–response relationship for the light-induced conductance changes for the three phases of the light response: the initial transient (circles), the later plateau (squares) and the DAP (triangles). The open symbols correspond to a photoreceptor after 15 min of dark adaptation, $V_{rest}=-67$ mV. Dark conductance (G_o) was 50 nS. The solid symbols correspond to a photoreceptor (from a different preparation) after 50 min in the dark. $V_{rest}=-71$ mV, $G_o=74$ nS. The inset shows the recordings used to measure the membrane conductance (see Materials and methods) for the three increasing light intensities (from top to bottom) for the photoreceptor represented by the solid symbols. The lower record in the inset (L) corresponds to the light pulse.

detected, as illustrated in Fig. 4. The insets of Fig. 4 show the voltage deflections in response to small hyperpolarizing current pulses of 0.33 nA and 100 ms, superimposed on the light responses, and show that a membrane conductance increase occurred during the light response.

The curves in Fig. 4 show the relationship between the conductance increase during the three phases of the light response (initial transient, plateau and DAP) and the light intensity on a logarithmic scale (a G_m–log$I$ curve). The ordinate is normalized for the maximal conductance value attained during the light response, usually the initial transient. This graph shows the relationship between both variables for two photoreceptors subjected to different dark-adaptation times. For a longer adaptation the conductance–intensity curves shifted to the left, towards lower intensities, on the log$I$ axis; that is, the longer the time in the dark, the lower the light intensity necessary to reach a given conductance increase. As in the case of the V–log$I$ curve (see Fig. 1), the dependence on light intensity was steeper for the initial transient than for the two other phases.

The time course of the membrane conductance change during the entire light response, including both the transient and the plateau phases, is shown in Fig. 5.
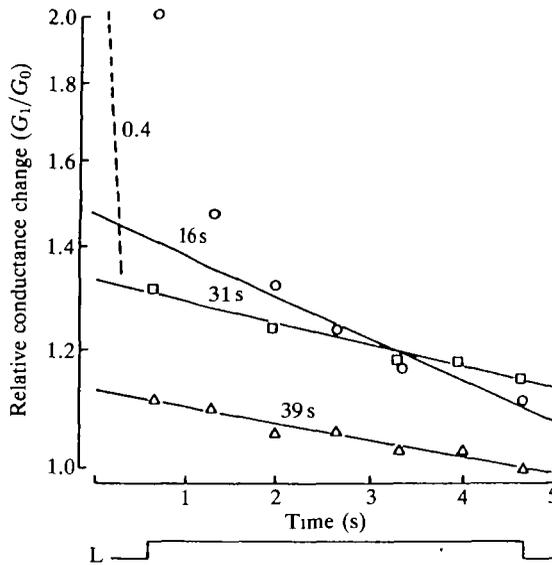
Fig. 5. The time course of the conductance changes in a photoreceptor cell in response to light stimuli of increasing intensity. The ordinate is the relative conductance change on a logarithmic scale, measured as the ratio of the membrane conductance during the light response (G_1) to the conductance in the dark (pre-stimulation, G_0). At relatively low intensities the time course can be described by a single exponential decay, but for the highest intensity the time course has at least two exponential components, the faster one denoted by the dashed line. The figures above the lines are the time constants for each exponential. The corresponding intensities are (in $lx \times 10^2$): 26.4 ($\bigcirc$), 4.2 ($\square$) and 0.5 ($\triangle$), $G_0 = 53$ nS, 16°C. The lower trace (L) shows the time course of the light pulse.

The data are those obtained from the same cell used in Fig. 4 (open circles). For low intensities the conductance change followed a decaying time course described by one exponential component. For higher intensities at least two exponential components could be demonstrated.

Depolarizing afterpotential

One constant feature in most of the recordings obtained was the presence of a well-defined depolarizing afterpotential (DAP). The inset of Fig. 6 illustrates that, during the development of the DAP in the crayfish retinular cells, there was an incremented conductance that outlasted the light stimulus. However, when correlating membrane potential and conductance during the DAP, it was consistently found that the conductance increment was of shorter duration than the depolarization. The membrane conductance returned to the value in the dark in about 30–50 % of the total time course of the DAP. The triangles in Fig. 1 describe the dependence of the initial (maximal) depolarization level of the DAP on the stimulus intensity for the recordings showed in the inset. The dependence of the DAP on light intensity was similar to the dependence of the late plateau phase
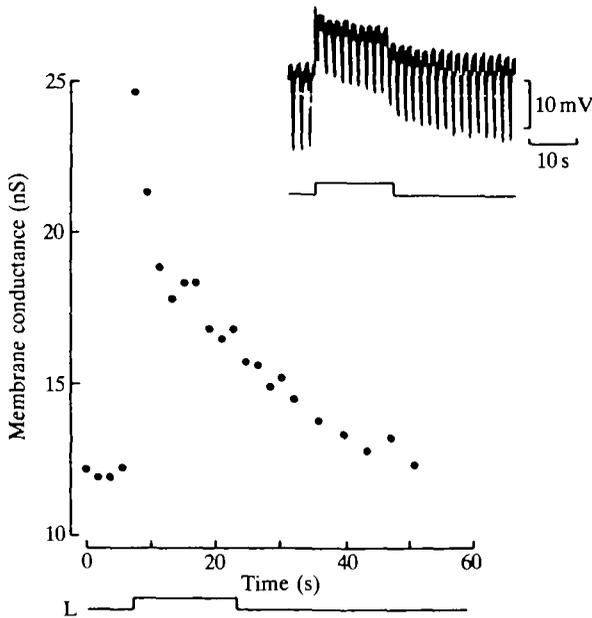
Fig. 6. Changes in membrane conductance during the depolarizing afterpotential (DAP) in a crayfish retinular cell. Graphic representation of the conductance change from the record shown in the inset. The voltage deflections are in response to hyperpolarizing current pulses (0.2 nA, not shown). The stimulus intensity is 4000 lx, and its time course corresponds to the lower trace (L).

of the RP. The dependence on light intensity of the maximal (initial) conductance change during the DAP is shown in Fig. 4 (triangles) for two photoreceptors in different states of dark adaptation. As in the case of the two other components of the light response, the light-dependence of the membrane conductance during the DAP was shifted to the left for longer adaptation times.

Discussion

As for many other photoreceptors, the V–log$I$ curve is adequately described by the hyperbolic relationship represented by equation 1. The values obtained for the exponent n were close to 1.0, as previously reported for this species (Glantz, 1968, 1972; Cummins and Goldsmith, 1986), for another crustacean (0.85 for *Ligia*, Shaw and Stowe, 1982) and for the locust (0.5–1.0, Matic and Laughlin, 1981). This value is greater than those reported for other invertebrate retinular cells (Wu and Pak, 1978; Tsukahara and Horridge, 1977; Eguchi and Horikoshi, 1984).

The range of values for V_{rest} reported here is similar to that in other invertebrate photoreceptors. The mean value (49.8±3.3 mV; mean±s.E., see Table 1) is towards the upper limit of the range reported previously for crayfish photorecep-tors (Eguchi, 1965; Nosaki, 1969; Waterman and Fernández, 1970; Muller, 1973;

Stieve et al. 1977; Bryceson and McIntire, 1983; Bryceson, 1986). This is possibly due to the finer pipette tips used in our recordings.

The shape of the I–V relationship is also similar to that described for other invertebrate photoreceptors (Baumann, 1968; Millecchia and Mauro, 1969; Lisman and Brown, 1971; Brown et al. 1970, 1971; Hudspeth et al. 1977). It displays some rectification. In these reports the membrane resistance is lower for the depolarizing than for the hyperpolarizing range with respect to V_{rest}. The same is true for our results (see Fig. 2).

For a simple geometrically shaped photoreceptor, a smooth-surfaced regular cylinder with typical dimensions (150 μm long, 15 μm in diameter, after Eguchi et al. 1973; Muller, 1973), the total membrane area is about 7000 μm^2. However, the effective surface membrane area is much greater owing to the contribution of the membrane evaginations forming the rhabdomeric microvilli. A more realistic estimate of the effective membrane surface area is 91 000 μm^2 including soma, microvilli and axon membranes (Krebs, 1974). The value experimentally obtained for total capacitance in our samples is 3.2±0.5 nF. Some of the geometrical estimation may have an error factor of 2 or 3. The value of R_m should be taken as a lower limit, but it could well be 2–3 times larger, and the value obtained for C_m 2–3 times lower. This latter value would be in close agreement with the usual one of 1 μF cm^{-2}, which appears to be relatively constant in biological membranes. As reported for other types of invertebrate photoreceptor, the value obtained here for R_m was typically larger than in other cell membranes. Hudspeth et al. (1977) have proposed this feature as an intrinsic property of the photoreceptor membranes. Our results support this hypothesis for the crayfish retinular cells. This characteristic enables the photoreceptor to propagate signals with low decrement along their entire length, with space constant values comparable to their actual size.

The isopotentiality of the cell interior suggests a lack of electrical coupling between the photoreceptor cells in the crayfish retina. This is still a controversial issue; electrical coupling has been proposed in the crayfish retinal photoreceptors (Muller, 1973). However, no dye-coupling between neighbouring crayfish photoreceptors has been found (Cummins and Goldsmith, 1981) and no gap junctions could be observed when specifically examined (Fernández and Nickel, 1976). Having a precise cable model of photoreceptors could provide a new insight into this problem.

The results presented in this paper show that, as in the other invertebrate photoreceptors studied, the RP of crayfish retinular cells corresponds to a transient increase of membrane conductance. The existence of two first-order components in the time course of this conductance increase in response to light suggests the existence of at least two distinct kinetic processes. Given the long time required to charge the membrane capacitance, we cannot rule out with our method the possible existence of more than two kinetic processes. Only the direct recording of membrane currents under voltage clamp will clarify this issue.

The DAP has never been analysed in crayfish photoreceptors but it is possible to

observe it in previous records (Eguchi, 1965; Glantz, 1968; Bryceson, 1986; Cummins and Goldsmith, 1986). The light-dependence of the DAP is similar to that of the late plateau of the RP (Fig. 1). However, membrane conductance during the DAP is still greater than that in the dark, but only during the initial part (30–50 %) of the total DAP. The remaining part of the DAP could be only a residual depolarization that returns spontaneously to the equilibrium potential of the most permeable ion in the dark (most probably potassium). It has been suggested that the prolonged afterdepolarization is a continuation of the same process(es) causing the RP (a change in membrane conductance) and is presumably related to long-lived products of photopigment breakdown (for a review see Hillman *et al.* 1983). Our results could be interpreted as agreeing with this proposition. At any rate, the nature of the conductance(s) responsible for this prolonged after-response remain(s) to be elucidated.

References

ARÉCHIGA, H., BAÑUELOS, E., FRIXIONE, E., PICONES, A. AND RODRÍGUEZ-SOSA, L. (1990). Modulation of crayfish retinal sensitivity by 5-hydroxy-tryptamine. *J. exp. Biol.* 150, 123–143

ARÉCHIGA, H. AND HUBERMAN, A. (1980). Hormonal modulation of circadian rhythmicity in crustaceans. In *Frontiers of Hormone Research*, vol. 6, *Comparative Aspects of Neuroendocrine Control of Behavior* (ed. C. Valverde and H. Aréchiga), pp. 16–34. S. Karger AG.

BAUMANN, F. (1968). Slow and spike potentials recorded from retinula cells of the honeybee drone in response to light. *J. gen Physiol.* 52, 855–875.

BROWN, H. M., HAGIWARA, S., KOIKE, H. AND MEECH, R. W. (1970). Membrane properties of a barnacle photoreceptor examined by the voltage clamp technique. *J. Physiol., Lond.* 208, 385–413.

BROWN, H. M., HAGIWARA, S., KOIKE, H. AND MEECH, R. W. (1971). Electrical characteristics of barnacle photoreceptors. *Fedn Am. Socs exp. Biol.* 30, 69–78.

BRYCESON, K. P. (1986). Diurnal changes in photoreceptor sensitivity in a reflecting superposition eye. *J. comp. Physiol.* 158, 573–582.

BRYCESON, K. P. AND McINTIRE, P. (1983). Image quality and acceptance angle in a reflecting superposition eye. *J. comp. Physiol.* 151, 367–380.

CAECI, M. S. AND CACHERIS, W. P. (1984). Fitting curves to data. The Simplex algorithm is the answer. *Byte* 9, 340–362.

CUMMINS, D. AND GOLDSMITH, T. H. (1981). Cellular identification of the violet receptor in the crayfish eye. *J. comp. Physiol.* 142, 199–202.

CUMMINS, D. AND GOLDSMITH, T. H. (1986). Responses of crayfish photoreceptor cells following intense light adaptation. *J. comp. Physiol.* A 158, 35–42.

EGUCHI, E. (1965). Rhabdom structure and receptor potentials in single crayfish retinular cells. *J. cell. comp. Physiol.* 66, 411–430.

EGUCHI, E. AND HORIKOSHI, T. (1984). Comparison of stimulus–response (*V*–log*I*) functions in five types of lepidopteran compound eyes (46 species). *J. comp. Physiol.* 154, 3–12.

EGUCHI, E., WATERMAN, T. H. AND AKIYAMA, J. (1973). Localization of the violet and yellow receptor cells in the crayfish retinula. *J. gen. Physiol.* 62, 355–374.

FAIN, G. L. AND LISMAN, J. E. (1981). Membrane conductances of photoreceptors. *Prog. Biophys. molec. Biol.* 37, 91–147.

FERNÁNDEZ, H. R. AND NICKEL, E. E. (1976). Ultrastructural and molecular characteristics of crayfish photoreceptor membranes. *J. Cell Biol.* 69, 721–732.

FUORTES, M. G. F. (1963). Visual responses in the eye of the dragonfly. *Science* **142**, 69–70.

GLANTZ, R. M. (1968). Light adaptation in the photoreceptor of the crayfish, *Procambarus clarkii*. *Vision Res.* **8**, 1407–1421.

GLANTZ, R. M. (1972). Visual adaptation: a case of non-linear summation. *Vision Res.* **12**, 103–109.

HILLMAN, P., HOCKSTEIN, S. AND MINKE, B. (1983). Transduction in invertebrate photoreceptors: role of pigment bistability. *Physiol. Rev.* **63**, 668–772.

HUDSPETH, A. J., POO, M. M. AND STUART, A. E. (1977). Passive signal propagation and membrane properties in median photoreceptors of the giant barnacle. *J. Physiol., Lond.* **272**, 25–43.

KREBS, W. (1974). Area and volume relationship in the crayfish retina. *Vision Res.* **14**, 441–442.

LAUGHLIN, S. (1981). Neural principles in the peripheral visual systems of invertebrates. In *Handbook of Sensory Physiology*, vol. VII/6B (ed. H. Autrum), pp. 133–280. Berlin: Springer-Verlag.

LISMAN, J. E. AND BROWN, J. E. (1971). Two light-induced processes in the photoreceptor cell of *Limulus* ventral eye. *J. gen. Physiol.* **58**, 544–561.

MATIC, T. AND LAUGHLIN, S. B. (1981). Changes in the intensity–response function of an insect's photoreceptors due to light adaptation. *J. comp. Physiol.* **145**, 169–177.

MILLECCHIA, R. AND MAURO, A. (1969). The ventral photoreceptor cells of *Limulus*. III. A voltage-clamp study. *J. gen. Physiol.* **54**, 331–351.

MULLER, K. J. (1973). Photoreceptors in crayfish compound eye: electrical interactions between cells as related to polarized-light sensitivity. *J. Physiol., Lond.* **232**, 573–595.

NAKA, K. I. AND EGUCHI, E. (1962). Spike potential recorded from the insect photoreceptor. *J. gen. Physiol.* **45**, 663–680.

NAKA, K.-I. AND KUWABARA, M. (1959). Two components from the compound eye of the crayfish. *J. exp. Biol.* **36**, 51–61.

NAKA, K. I. AND RUSHTON, W. A. H. (1966). S-potential from colour units in the retina of fish (Cyprinidae). *J. Physiol., Lond.* **185**, 536–555.

NOSAKI, H. (1969). Electrophysiological study of color encoding in the compound eye of crayfish *Procambarus clarkii*. *Z. vergl. Physiol.* **64**, 318–323.

PICONES, A. AND ARÉCHIGA, H. (1985). Electrical properties of crayfish photoreceptor cells. *Biophys. J.* **47**, 474a.

SHAW, S. R. AND STOWE, S. (1982). Photoreception. In *The Biology of Crustacea*, vol. 3 (ed. H. L. Atwood and D. C. Sandeman), pp. 291–367. New York: Academic Press.

STIEVE, H., BOLLMANN-FISCHER, H. AND BRAUN, B. (1971). The significance of metabolic energy and the ion pump for the receptor potential of the crayfish photoreceptor cell. *Z. Naturforsch.* **26b**, 1311–1321.

STIEVE, H., BRUNS, M. AND GAUBE, H. (1976). Simultaneous recording by extra- and intracellular electrodes of light responses in the crayfish retina. *Vision Res.* **18**, 621–628.

STIEVE, H., BRUNS, M. AND GAUBE, H. (1977). Ability to light-induce conductance change of arthropod visual cell membrane, indirectly depending on membrane potential, during depolarization by external potassium or ouabain. *Z. Naturforsch* **32c**, 855–869.

TSUKAHARA, Y. AND HORRIDGE, G. A. (1977). Interaction between two retinula cell types in the anterior eye of the dronefly *Eristalis*. *J. comp. Physiol.* **115**, 287–298.

WATERMAN, T. H. AND FERNÁNDEZ, H. R. (1970). E-vector wavelength discrimination by retinular cells of the crayfish *Procambarus*. *Z. vergl. Physiol.* **68**, 154–174.

WU, C. F. AND PAK, W. L. (1978). Light-induced voltage noise in the photoreceptor of *Drosophila melanogaster*. *J. gen. Physiol.* **71**, 249–268.